26th ABCM International Congress of Mechanical Engineering
November 22-26, 2021. Florianópolis, SC, Brazil

INFLUENCE OF GEOMETRIC PARAMETERS ON THE PIEZOELECTRIC RESPONSE OF THIN PVDF FILMS EXCITED BY LONGITUDINAL MECHANICAL STRESS WAVES

Luiz Felipe de Oliveira Marchezini
lipeolimarche94@gmail.com

Suchilla Garcia Leão
suchilla.garcia@gmail.com

Antônio Ferreira Ávila
avila@demec.ufmg.br

Antônio Augusto Torres Maia
aamaia@ufmg.br

Graduate Program in Mechanical Engineering
Federal University of Minas Gerais,
Av. Pres. Antônio Carlos, n° 6627

Abstract *Films made of polyvinylidene difluoride (PVDF), when coated with silver ink, constitute piezoelectric sensors that can detect and measure in-plane stress waves in structures. These films can be cut with different geometrical dimensions, and the final film shape can influence its frequency response curve. The objective of this article is to evaluate the influence of geometrical dimensions of PVDF film sensors on its electrical response when attached to a thin bar exposed to in-plane sinusoidal stress waves. To develop this analysis, a mathematical model was used to simulate the mechanical excitation, the piezoelectric response of the sensor, the relation between the excitation frequency and output electrical impedance, and its impact over the signal obtained using typical electrical measurement equipment like an oscilloscope or voltmeter. Results showed that reductions on sensor length to one third of its original size triplicated the frequency bandwidth suitable for measurements. It also significantly increased the higher cut-off frequency, making it suitable for measurement of stress waves with higher frequencies. Simulations related to an electrical output impedance of this sensor showed that the loading effect can significantly affect signal amplitude over the frequency range. For standard PVDF sensor and typical electrical measurement equipment, with 1MΩ of electrical input impedance, the attenuation of the signal at 1 Hz can be higher than -40 dB and the lower cut-off frequency of the system higher than 200 Hz. Such factor, if not considered, can generate errors related to the measurement of the magnitude of stress waves with lower frequencies.*
Keywords: *piezoelectric, polymer, sensor, mathematical, model.*

1. INTRODUCTION

Piezoelectric polymers are one type of material into which modern science have been interested. This material unites some polymeric properties, like moldability, high flexibility, tenacity and small volumetric density with piezoelectric ones, fast electromechanical response, small energy level to activation and possibility of use over a broad frequency spectrum. These characteristics makes this material useful for development of sensors to structural sensing and monitoring.Such field has scientific and professional relevance, once it is present on equipment operation, manufacturing processes, explosions and collisions. Over all the scientific work that studies the response of PVDF thin film sensors to longitudinal stress waves propagating on a structure, work published by Brown (1990) and articles written by Kotian(2013a) and Kotian *et al*(2013b) stand out. The first one presents a qualitative and semi quantitative analyses of the response of this sensor to longitudinal stress waves propagating on a bar, while the second one numerically modeled this physical situation and the third one experimentally measured the response of this sensor to dynamic mechanical stimuli. On these works, a critical parameter that affects the piezoelectric response to mechanical stress waves is the geometry of the sensor. Brown (1990) indicated that this parameter is directly related to the attenuation of the response of the sensor on high frequencies. Kotian(2013a) related the amplitude of the piezoelectric response to the length and thickness of the sensor. Such results are relevant and contribute to the understanding of the phenomenon. However, the analysis used presents some gap. In these works, the electric behavior of the sensor is not

considered. This component, due to its own material constitution and geometry, has electrical characteristics that can influence the signal generated by the sensor and, therefore, should be considered.

The contribution of this paper for the area is the improvement of the work developed by the above mentioned authors with the inclusion of an electric model of the sensor into which the parameters are connected to the proper geometry of the sensor. This electrical model, based in theories presented in work from Measurement Specialties (1999) and Texas Instruments(2001), and feed with values supported by experimental work published by Chang *et al* (2013) and Gusarov (2015), improves the capacity of piezoelectric sensor model for dynamic solicitation. As consequence of this improvement, it was possible to simulate the attenuation of the response of the sensor for mechanical solicitations with low frequencies due to the resistive-capacitive electrical nature of the sensor, generate frequency response curves for sensors with different geometric parameters and also analyze the *loading effect* presented by the sensor when its directly coupled to a measurement equipment with low input impedance.

2. METHODOLOGY

The electrical model (Figure 1) used in this paper is based on a simple piezoelectric sensor, represented by a voltage source in series with an electrical impedance composed by a capacitor in parallel to a resistor (Texas Instruments, 2001). In series with the sensor, the electric circuit of the input resistance of the measurement equipment is represented by a resistor (Kotian, 2013b). On this model, V_{in} is a parameter that represents the electric voltage generated by the piezoelectric effect of the sensor due to stress waves propagating in the structure where it is hosted. C_{sensor} is a parameter that represents the sensor capacitance due to its constitution and geometric format. It follows the parallel plate capacitor model, presented by Measurement Specialties (1999). The insulation characteristics of the sensor due the material properties are represented by the electrical resistance R_{sensor}. Its value was estimated with use of Ohm's second law, which calculated result, when confronted with experimental results from Gusarov (2015) and Chang *et al* (2013), presented a value with same order of magnitude. The electric circuit of the input resistance of the measurement equipment is represented by a resistor ($R_{oscilloscope}$), which value can be obtained from datasheet of specific measurement equipment used. The last parameter, V_{out} ,represents the numerical value of the signal read by the measurement equipment. It is assumed that the properties of the sensor and structure do not change with frequency or temperature.

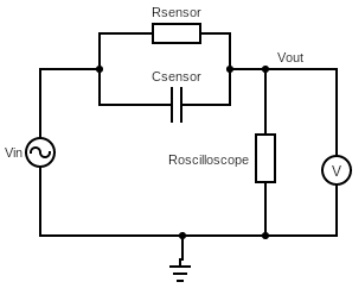

Figure 1: Equivalent electrical circuit diagram

2.1 Piezoelectric behavior of PVDF sensor

To correctly describe the piezoelectric behavior of the PVDF sensor, it is necessary to consider the direction which the mechanical effort is applied and also the direction in which the electrical response is monitored. Figure 2 shows a PVDF film positioned over a Cartesian coordinate system composed of three orthogonal directions. The length of the film is parallel to the longitudinal direction (1), the width is parallel to the transversal direction (2) and the thickness is parallel to the normal direction (3).

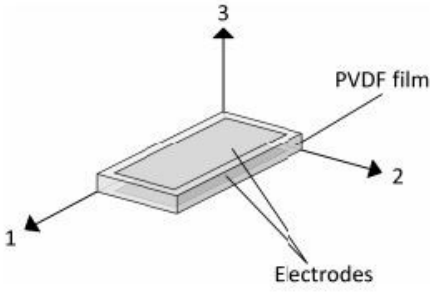

Figure 2: Diagram showing PVDF sensor's axes
(Kotian *et al,* 2013)

Considering Figure 2, one of the linearized coupled constitutive set of equations for piezoelectric behavior that can be used to describe the coupling between mechanical strain (S), mechanical stress (T), electric field (E), and electric displacement (D) presented by this material are presented in Equations (1) and (2) (Kotian *et al*, 2013).

$$S_p = \overset{D}{s}_{pq} T_q + g_{kp} D_k, \tag{1}$$

$$E_i = g_{iq} T_q + \overset{T}{\beta}_{ik} D_k, \tag{2}$$

Where s is the compliance, g is the piezoelectric voltage coefficient and β is the inverse dielectric constant. The superscripts D and T refer to specific conditions of measurement of s (s^D – compliance measured at zero electric displacement) and β (β^T – the inverse of dielectric constant measured at zero stress). The subscripts p and q are compressed matrix notations and can have values from 1 to 6, representing 11, 22, 33, 23 or 32, 31 or 13, and 21 or 12 directions. The subscripts i and k are general notations with values from 1 to 3, representing 1,2 and 3 directions, as defined in Figure 2.The constitutive set of equations presented in Equations (1) and (2) can be simplified due to the structural symmetry of piezoelectric materials, a factor that makes null many compliance, dielectric and piezoelectric coefficients (Gusarov, 2015). Considering that the commercial PVDF film presents, in its structure, biaxial preferential orientation, only the piezoelectric voltage coefficients g_{31}, g_{32}, g_{33}, g_{15} and g_{24} are not null (Harrison and Ounaies, 2001). Considering both simplifications, strain along the longitudinal direction (S_1) and electric field along the normal direction (E_3) are related by Equations (3) and (4):

$$S_1 = \overset{D}{s}_{11} T_1 + \overset{D}{s}_{12} T_2 + \overset{D}{s}_{13} T_3 + g_{13} D_3, \tag{3}$$

$$E_3 = g_{31} T_1 + g_{32} T_2 + g_{33} T_3 + \overset{T}{\beta}_{33} D_3, \tag{4}$$

Considering now that electric field (E) will be measured along PVDF thickness direction (3) with an equipment with sufficient high resistance to avoid current flow through the electrodes, D_3 can be considered null and the previous set of equations are simplified to :

$$S_1 = \overset{D}{s}_{11} T_1 + \overset{D}{s}_{12} T_2 + \overset{D}{s}_{13} T_3, \tag{5}$$

$$E_3 = g_{31} T_1 + g_{32} T_2 + g_{33} T_3, \tag{6}$$

Considering that PVDF thin film thickness is some orders of magnitude smaller than its width and length, the relation between the electric field (E) and electric voltage (V) can be approximated to the model of a parallel plate capacitor, as described in Equation (7).

$$E = \frac{V}{h}, \tag{7}$$

where h denotes the distance between planes on the thickness direction of the PVDF thin film. The use of the relation presented in Equation (7) on Equation (6) generates an equation that correlates mechanical tension components that actuate on the PVDF film and the electric potential generated on thickness direction by the sensor (shown in Eq. (8)).

$$V_3 = h \cdot \left(g_{31} T_1 + g_{32} T_2 + g_{33} T_3 \right), \tag{8}$$

If the mechanical solicitation plane stress characteristics, as in plane stress solicitations, mechanical stress on the normal direction can be considered null and Eq. (8) is further simplified to Eq. (9), presented below

$$V_3 = h \cdot \left(g_{31} T_1 + g_{32} T_2 \right), \tag{9}$$

2.2 Voltage Source Element

The results obtained so far indicated that the electrical voltage generated between electrodes on thickness direction (3) is proportional to the stress amplitude acting on the sensor in longitudinal (1) and transversal (2) directions.

Equations developed in the previous section are initially local, valid for each point comprehended inside the sensor region. Considering that the piezoelectric response of PVDF sensors to mechanic solicitation occurs over its whole volume, the electrical signal presented on its conductive electrodes is a sample of all piezoelectric response of PVDF to local mechanical solicitation actuating on the sensor. (Brown, 1990), (Zhang *et al*, 1993) and (Kotian *et* al, 2013b) models the piezoelectric response of PVDF film sensor as an electrical signal proportional to the averaged value of mechanical efforts actuating on sensor coated surface area. To better indicate this approach, a piece of Kotian *et al* work is reproduced below:

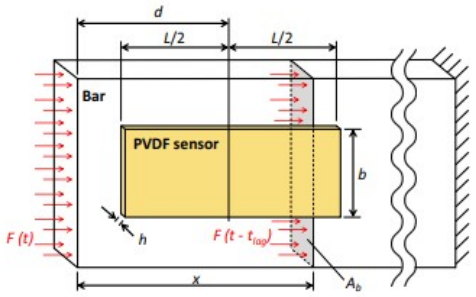

Figure 3: Physical model of PVDF thin film sensor exposed to longitudinal stress wave propagation. Kotian *et al*, 2013.

Kotian *et* al (2013b) considered a PVDF thin film bonded to a thin bar with one end subjected to a uniformly distributed force and the other fixed, as presented in Figure 3. The PVDF thin film coated with silver ink has length *L*, width *b,* and thickness *h*. Its center is located at a distance *d* from the free extremity, where periodic uniform sinusoidal force *F(t)* is applied over the surface area of this extremity of the bar (A_{bar}). This force propagates through the thin bar as a wave with a velocity c_0, with its front acting on a point, distanced *x* from the free end after a time represented as t_{lag}. To analyze this physical situation, the authors assumed some considerations:

- 1º - PVDF and material of the bar are perfectly elastic, with strain and stress following the relation $E.\varepsilon_x = \sigma_x$;
- 2º - Bonding between the film and the structure are perfect, so the normal strain generated in structure due to external mechanical force F(t) is completely transferred to the PVDF thin film. ($\varepsilon_{x\ bar} = \varepsilon_{x\ PVDF\ thin\ film}$) ;
- 3°- The compressive force F(t) is uniformly distributed and applied at one of the extremities (free one);
- 4º - The effect of wave reflection at the bar's ends is ignored;
- 5° - Stress waves components into transversal (T_2) and normal (T_3) directions are considered null;
- 6º - PVDF stiffness are considered null when compared to the structure stiffness and not affect the global stiffness of the system when the pressure is applied at on of the extremities;

Using these considerations over the proposed physical situation, Kotian *et al*(2013b) develops a mathematical analysis that shows that, for a longitudinal stress wave (T_{bar}) propagating through the material with velocity c_0 as sinusoidal wave with circular frequency ω, as presented by Equation (10),

$$T_{\text{bar}}(x,t)=\frac{F}{A_{\text{bar}}}\cdot\sin\left(2\cdot\pi\cdot f\left(t-\frac{x}{c_0}\right)\right)=\frac{F}{A_{\text{bar}}}\cdot sin\omega\left(t-\frac{x}{c_0}\right)=\sigma_{\text{bar}}\cdot sin\omega\left(t-\frac{x}{c_0}\right), \tag{10}$$

the electric voltage generated by the PVDF sensor is:

$$V_{3\,Avg}(t)=\left(\frac{h\cdot g_{31}\cdot E_{sensor}\cdot F\cdot c_0}{E_{\text{bar}}\cdot A_{\text{bar}}\cdot\pi\cdot f\cdot L}\right)\sin\left(\frac{\pi\cdot f\cdot L}{c_0}\right)sin\omega\left(t-\frac{d}{c_0}\right), \tag{11}$$

2.3 Capacitance Element

As presented earlier, the equivalent model used to describe the PVDF thin film electric capacitance is the parallel plate capacitor one. The application of this model into the PVDF thin-film sensor considers the electrodes deposited over faces oriented in the normal direction (3) as the parallel plates, while the PVDF thin film is considered the dielectric insulating both faces. The equivalent diagram of this capacitance is presented in Figure 4.

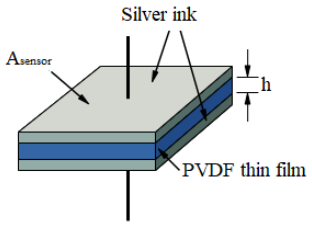

Figure 4: Diagram of Parallel Plate Capacitor applied to PVDF thin film coated with silver ink

The mathematical equation that correlates the geometric parameters of the PVDF thin film with its electrical capacitance is, by the use of this model, equivalent to the relation presented in Equation (12).

$$C = \frac{\varepsilon \cdot \varepsilon_0 \cdot A_{sensor}}{h} = \frac{\varepsilon \cdot \varepsilon_0 \cdot L \cdot w}{h}, \tag{12}$$

where ε refers to PVDF relativity permittivity, ε_0 refers to the permittivity of vacuum, A is the active area of the electrode and h is the PVDF film thickness.

2.4 Resistive Element

The equivalent resistive element of a piezoelectric sensor model is related to the leakage current that flows through the element due to its intrinsic limited insulating resistance. In order to estimate the equivalent electrical resistance from this sensor, Ohm's law was used and the result was confronted with experimental data presented in works of Chang *et al*(2013) and Gusarov (2015). It was observed that, for dimensions presented by the commercial PVDF film LDT1-028K, manufactured by Measurement Specialties, the model and experiments presented values obtained were from same order of magnitude. Ohm's law is presented in Equation (13).

$$R_{\text{Sensor}} = \frac{\rho \cdot h}{L \cdot w}, \tag{13}$$

2.5 Equivalent AC Electrical Circuit

If the results presented in sections 2.1, 2.2, 2.3 and 2.4 are unified using the electrical model proposed by Texas Instruments (2001), it is possible to use the model to simulate PVDF thin film response to longitudinal stress wave with specified amplitude and frequency. To do so, an Alternating Current (AC) analysis will be adopted. To evaluate the electrical voltage read by the oscilloscope, it will be assumed that the transient response due to initial conditions has already decayed. For this case, the steady-state solution can be used to estimate V_{out} based on voltage division on the circuit due to electrical resistance and capacitive reactance. To analyze magnitude and phase, the method will use phasor representation. With this method, V_{in}, will be represented as:

$$V_{\text{in}} = \left|V_{3\,Avg}\right| \angle -w \cdot \frac{d}{c} = |V| \angle \theta, \tag{14}$$

while resistances and capacitive reactance will be represented as Equations (15), (16) and (17).

$$R_{\text{Oscilloscope}} = \left|R_{\text{Oscilloscope}}\right| \angle 0°, \tag{15}$$

$$R_{\text{sensor}} = \left|R_{\text{sensor}}\right| \angle 0°, \tag{16}$$

$$Z_c = \left|\frac{1}{2 \cdot \pi \cdot f \cdot C}\right| \angle -90° = |\text{Xc}| \angle -90°, \tag{17}$$

Using notations presented on Equation (15), (16) and (17) on the equivalent electric circuit diagram (Figure 1), the output impedance of piezoelectric sensor, Z_S, can be represented as Equation (18):

$$Z_s = R_{\text{sensor}} // Z_c, \tag{18}$$

while V_{out}, electrical voltage read by the oscilloscope, is

$$\left|V_{\text{out}}\right| \angle \phi = \frac{V_{\text{in}} \cdot R_{\text{Oscilloscope}}}{R_{\text{Oscilloscope}} + Z_s}, \tag{19}$$

3. RESULTS

The model presented in the previous section was used to generate the theoretical frequency response curve of piezoelectric PVDF films to mechanical propagating sinusoidal waves. Equation (19) was solved for a wide frequency range and, for each simulation, the result was modularized, multiplied by a constant in order to present, at its maximum, a value equal to one. After this treatment, the results were plotted as frequency curves responses diagrams, as can be seen in Fig. (5) to Fig. (10). The analysis of these figures allows the evaluation of specific behavior of PVDF sensors when exposed to a mechanical stimulus with different frequencies. The mathematical model has, in its constitution, variables that represent the geometrical dimensions of the sensor. Such parameters, present in Equations (11), (12), and (13), affect the amplitude of the measured voltage given by Equation (19). Using this approach, it was possible to change the value of these parameters over a specific range and visualize its influence on the frequency response curves of the sensor. The input impedance of the measurement equipment was also considered in the model. This parameter, represented in Equation (15), also influences the measured voltage given by Equation (19). The change of such parameter allowed the observation of *loading effect* interference into the electrical signal collected by the measurement equipment. To develop this study, a PVDF sensor with constant geometric dimensions and properties was assumed and frequency response curves were generated considering many input impedance of the measurement equipment.

3.1 Evaluation of frequency response for a standard PVDF film

For the conditions stipulated by the model developed in the previous section, considerating that the simulated PVDF sensor has the same properties and geometrical dimensions of the commercial PVDF sensor LDT1-028K, manufactured by Measurement Specialties, and that the measurement equipment has a pure resistive input impedance of 10MΩ, the theoretical frequency response curve of this sensor was calculated over the frequency range of 1Hz to 1.10^6 Hz. The results are presented in Figure (5).

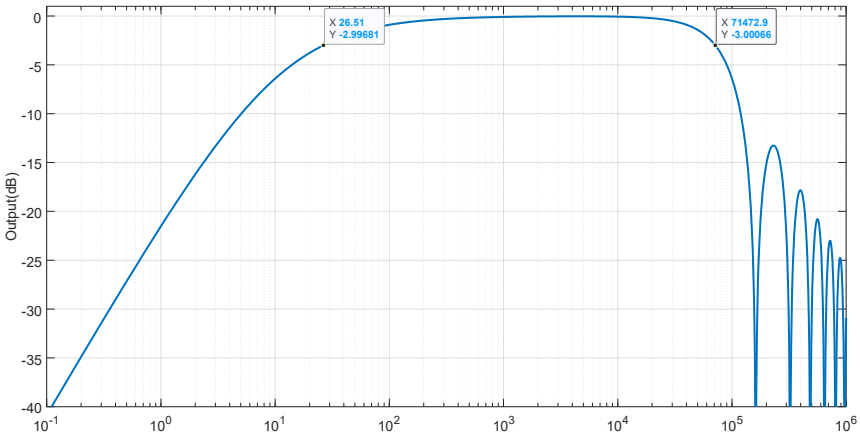

Figure 5: Theoretical Frequency response curve for PVDF film sensor with thickness 28um, length of 32mm and width of 12 mm. Equipment Input impedance of 10 MΩ.

The cut-off frequency is the frequency into which the frequency response presents an attenuation of 3dB. Figure 5 can be divided into three different regions: The first region, situated between the initial frequency simulated (0,1Hz) and first cut-off frequency (26,51 Hz), represents an attenuation region created by the RC filter due to the output impedance of the PVDF sensor: For low frequencies, the sensor presents high output impedance. Such impedance can be higher than the proper input impedance of the measurement equipment, which can cause a relevant attenuation in the piezoelectric response of the sensor to the mechanical solicitation. The second region, the intermediate one, localized between the first (26,51 Hz) and the second cut-off frequency (71,473 kHz), represents a region into which the

attenuation of the piezoelectric signal is low, with attenuation modulus lower than 3dB. The third region, localized after the second cut-off frequency (71,473 kHz), represents the region where the *roll-off* phenomenon occurs. This phenomenon, initially evaluated by Brown (1990) and posteriorly mathematically presented by Kotian (2013a), exists due to the interaction between the geometry of the sensor and the characteristics of the sinusoidal propagating wave. To better comprehend this behavior, the nature of Equation (11) must be considered: it contains the function sinc ($\pi fL/c_0$). The sinc function has, as a basic characteristic, its zeros located where the argument is an integer multiplied to π. In the physical model proposed, the argument of this function will be an integer when the length of the sensor is an integer multiple of the wavelength of the propagating wave on the bar. If the stress wave has a frequency higher than the higher cut-off frequency and enter on this region, it will be intensely attenuated. For sensing purposes, such region must be avoided, once it can significantly attenuate and distort signal generated by mechanical input signal composed of multiple high-frequency harmonics.

3.2 Influence of the geometric dimensions in the frequency response

If the amplitude calculated from Equation (19) is evaluated over the frequency spectrum for PVDF sensors with different lengths, the respective frequency response curves will be significantly affected. As can be seen in Figures 6 and 7, the frequency bandwidth located between cut-off frequencies is sensibly altered with the variation of the sensor length. In Figure 6, where the simulated sensor has its length reduced to 10.6 mm (one-third of the standard size), the cut-off frequencies were increased from 26,51Hz to 79,81 Hz and from 71,472 kHz to 215,75 kHz. As a direct consequence, the frequency bandwidth was significantly increased. For Figure 7, where the simulated sensor has its length increased to 96 mm (three times its original size), the cut-off frequencies are reduced from 26,51 Hz to 8,81 Hz and from 71,5 kHz to 23,8 kHz. For this case, the frequency bandwidth is reduced to one-third from the original sensor simulated.

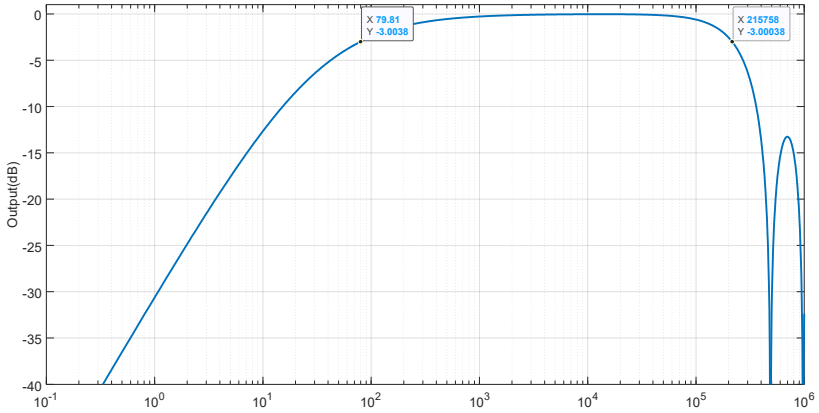

Figure 6: Theoretical Frequency response curve for PVDF film sensor with thickness 28 um, length of 10.6 mm and width of 12 mm. Equipment Input impedance of 10 MΩ.

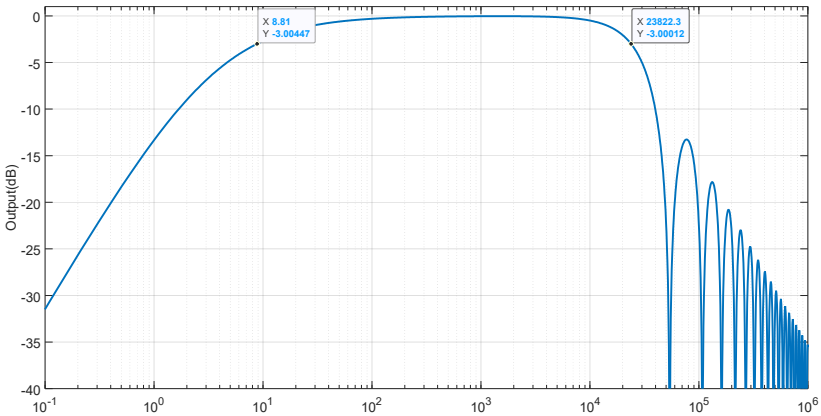

Figure 7: Theoretical Frequency response curve for PVDF film sensor with thickness 28 um, length of 96 mm and width of 12 mm. Equipment Input impedance of 10 MΩ.

The comparison between Figures 5, 6 e 7 indicate some relevan tendencies. The first one is the existence of an inverse relation between the length of the sensor and the absolute value of cut-off frequencies of the system: sensors with one third of the standard length presented, on its frequency curve response (Figure 6), cut-off frequencies values three times higher than sensors with standard length (Figure 5) and nine times higher than sensors with length three times bigger than the standard value (Figure 7). The second tendency identified is also an inverse relation between the length of the sensor and the frequency bandwidth of the system. Sensors with smaller length presented frequency curve response (Figure 6) with larger frequency bandwidth between cutoff frequencies than sensors with bigger length (Figure 7). Such results can be used as a guide to geometrically design sensors to be adequate to measure stress waves with frequency located inside a determined interval of frequencies. For the study of longitudinal stress waves with lower frequencies, can be interesting the use of sensors with bigger lengths, once they present lower cutoff frequencies. For the study of stress waves with higher frequencies, sensors with smaller lengths can be more adequate, once they have bigger cut-off frequencies and frequency bandwidth.

3.3 Influence of the input impedance of the measurement equipment into frequency response

In a measurement, proper coupling between the sensor and the measurement equipment is necessary for the proper quality of the measurement. One of the many factors that can affect its coupling and, therefore, the signal measured, is known as *loading effect*. This effect occurs due to the interaction between the electrical signal generated, the output impedance of the sensor, and the input impedance of the measurement equipment. Equation (19) indicates the numerical relation that exists between the parameters presented previously for the model adopted. To evaluate the influence of this interaction on the amplitude of the signal measured over a wide frequency spectrum, Equation (19) was evaluated for a sensor with geometrical dimensions and properties equal to the commercial sensor LDT1-028K while input impedance values from measurement equipment were altered. Figures 8, 9, and 10 represent the frequency response curves of the PVDF sensor for pure resistive input impedance equals to 1MΩ, 100MΩ e 1GΩ. The examination of Figures 5, 8, 9, and 10 allows the observation of the influence of input impedance into the frequency response curves of the PVDF sensors. For the lowest input impedance considered (1MΩ), the predicted attenuation of the signal for 1Hz (indicated by Figure 8) is nearly 40 dB and the lowest cut-off frequency is equal to 264 Hz. For input impedance of 10 MΩ and 100 MΩ, the signal attenuation at 1Hz is – 22 dB and -6 dB, respectively. The lowest cut-off frequency is, for these input impedance, 26,3 Hz and 2,5 Hz. For the highest input impedance considered, 1 GΩ, the signal attenuation at 1 Hz is almost negligible: 1dB. The cut-off frequency for this configuration is nearly 0,2 Hz.

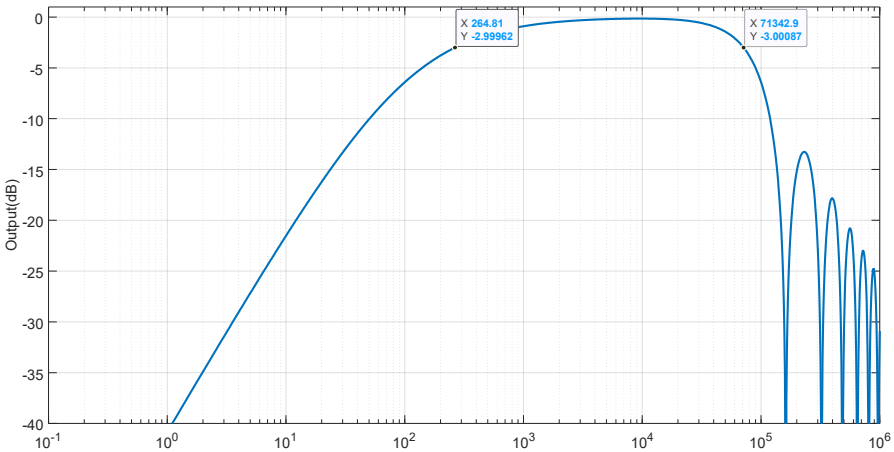

Figure 8: Theoretical Frequency response curve for PVDF film sensor with thickness 28um, length of 32mm and width of 12 mm. Equipment Input impedance of 1 MΩ.

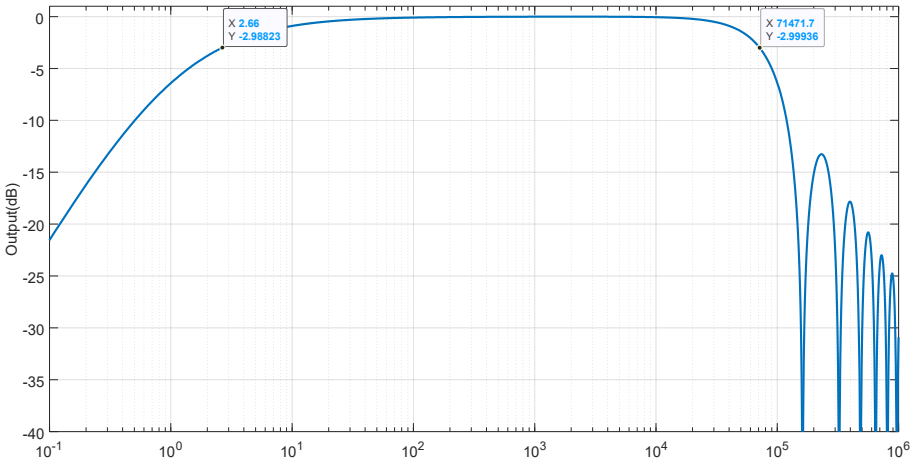

Figure 9: Theoretical Frequency response curve for PVDF film sensor with thickness 28um, length of 32mm and width of 12 mm. Equipment Input impedance of 100MΩ

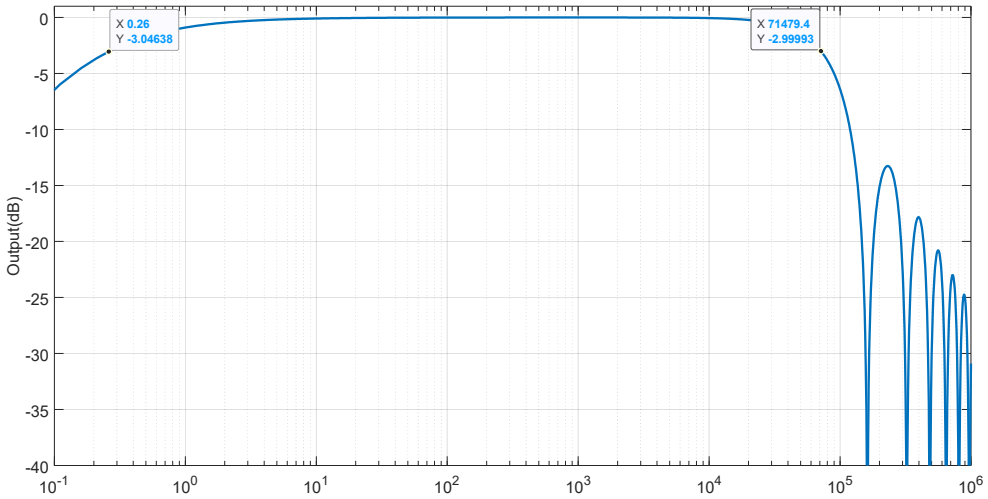

Figure 10: Theoretical Frequency response curve for PVDF film sensor with thickness 28um, length of 32mm and width of 12 mm. Equipment Input impedance of 1 GΩ.

Such results indicate that the response of this system to low frequencies is significantly affected by input electrical impedance of the measurement equipment. Comparison between Figures 5, 8, 9 and 10 allows the observation of the reduction of the lower cut–off frequency of the system for cases which the measurement equipment has higher electrical input impedance. This indicates the reduction of the *loading effect* as the input electrical impedance of the measurement equipment is increased. Form a practical point of view, it shows the necessity of consideration of such factor during selection of measurement equipment to avoid the attenuation due to *loading effect* on experimental measurements. For cases which stress waves are composed by low frequency harmonics, the inattention to such factor can result into the attenuation and distortion of the final signal collected.

4. CONCLUSION

The methodology and modeling adopted in this work allowed the simulation of the response of PVDF films to longitudinal stress waves propagating on a bar. Through them, it was possible to generate frequency response curves of this sensor, identifying the frequency range suitable for measurement, into which the attenuation modulus is lower than 3dB, and frequency ranges into which the response of the sensor is significantly attenuated due to the *loading effect* generated by its output impedance or the *roll-off* generated by the interaction between the geometry of the sensor and wavelength of the stress propagating on the bar.

By using the presented model it was possible to observe the influence of the sensor length in the frequency response curve of this component. The reduction of the sensor length generated an increase in the cutoff frequencies and frequency bandwidth. Such a result shows that the reduction of the length of the sensor can enlarge the bandwidth frequency into which the sensor can be used without been affected by meaningful attenuation. On the reverse direction,

the increase of the length of the sensor reduced cutoff frequency values and frequency bandwidth. This result indicate that the increment of the length sensor can allow the use of this sensor to detect propagating waves with lower frequencies. Both results can be used as basic references to choose the geometrical dimensions of the sensor in order to configure it to be sensible to a specific frequency range of stress waves propagating on the structure.

The model presented also allowed the observation of the influence of the input impedance of the measurement equipment into the frequency response curve. From these results, it can be noticed that measurement equipment with higher electrical input impedance are able to collect piezoelectric response of the sensor characterized by lower frequencies. This result can be useful in studies that are focused on the investigation of stress propagating waves with low-frequency harmonics.

5. ACKNOWLEDGEMENTS

This work was supported by Foundation for Research Support of the State of Minas Gerais (FAPEMIG), National Council for Scientific and Technological Development (CNPq) and Coordination of Improvement of Higher Level Personnel (CAPES).

6. REFERENCES

Brown, R.H., 1990, “Piezo Film : Form and Function”, Sensors and Actuators A: Physical, Vol. 22, Issues 1-3, pp. 729-733.

Cheng, W.Y., Hsu, C.H., Tsai, C.P., 2013, “Leakage and Fatigue Characteristics of Polyvynilidene Fluoride Film”.Applied Mechanics and Materials, Vol. 284-287, pp. 158-162

Gusarov, B., 2015,“PVDF piezoelectric polymers: characterization and application to thermal energy harvesting”. Doctoral Dissertation. University Grenoble Alpes

Harrison,J.S., Ounaies, Z., 2001, “Piezoelectric Polymers”, Contractor Report 2001-211422, NASA, https://ntrs.nasa.gov/api/citations/20020044745/downloads/20020044745.pdf . Accessed 14 June 2021.

Karki, J. “Signal Conditioning Piezoelectric Sensors”. Application Report SLO033A, Texas Instruments, https://www.ti.com/lit/an/sloa033a/sloa033a.pdf . Accessed 14 June 2021.

Kotian, K.,2013 “*Detection of In-Plane Stress Waves with Polyvinilidene Fluoride Sensors*”. Master Thesis, Graduate Program in Mechanical Engineering, The Ohio State University, Ohio, USA.

Kotian, K., Headings, L.M., Dapino, M. J., 2013. “Stress Averaging in PVDF sensors For In-Plane Sinusoidal and Impact Induced Stresses.” IEEE Sensors Journal, Vol. 13, No. 11, pp. 4444 – 4451.

Measurement Specialties, 1999, *Piezo Film Sensors Technical Manual*, Measurement Specialties Inc., Norristown, PA, https://mma.pages.tufts.edu/emid/piezo.pdf. Accessed 14 June 2021.

Zhang, H., Galea, S.C., Chiu, W. K., Lam, Y.C. ,1993, “An Investigation of thin PVDF films as fluctuating strain measuring and damage monitoring devices”. Smart Material Structure, Vol.2, pp. 208-216.

7. RESPONSIBILITY NOTICE

The authors are the only responsible for the printed material included in this paper.